SPACE TELESCOPE SCIENCE INSTITUTE
Operated for NASA by AURA

Instrument Science Report NICMOS 2008-003

Verifying the NICMOS Count Dependent Non-Linearity Correction

B. Shaw, R. S. de Jong
June 30, 2008

ABSTRACT

We re-investigate the NICMOS count dependent non-linearity, using the flat field lamps to reach high count regimes. The NICMOS count dependent non-linearity has been previously quantified and is currently corrected in NICMOS pipeline. In this document we show that the count dependent correction is still accurate to within 1.2% of true linearity for counts above 100 ADU independent of filter used. This is a response to the count-rate dependent non-linearity investigations, to eliminate questions about the current count dependent corrections.

Introduction

The NICMOS cameras detect counts non-linearly. This effect is typical for all IR detectors, and was quantified in Cycle 7 by fitting a second degree polynomial to the count detection for each pixel in long exposure flat field images. The count non-linearity is currently corrected through the standard calnica data pipeline. We revisit the count non-linearity to verify that it is still corrected to within 1.2% of linear count collection for counts greater than 100 ADU.

Data

Data from count rate non-linearity proposal 11062 and flat monitor programs 10728 and 11059 were used for this investigation. The non-linearity data consists of a sequence of images of a stellar cluster, NGC 3603, taken out of focus, followed with the same

sequence with the flat field lamp turned on, followed by darks. The lamp-on images provide artificially increased counts to verify the count correction in the high count regime.The dark frames taken immediately after the stellar cluster images were used in substitution of the calnica pipeline reference files to subtract the dark current. Similarly, the flat monitor data includes a matching set of long exposure, lamp off-on images for an empty field. The lamp-off frames taken before the flat field lamp was turned on, were used in substitution of the calnica pipeline reference files to subtract the dark current.

Table 1. Multiaccum data sets used for this investigation. Each set includes a combination of images with both the flat field lamp on and off for the same field and readout sequence.

Target	Rootname	Obs-Date	Camera	Filter
Pointed Flat	n6ki03	2002-07-16	1	F160W
Pointed Flat	n8i303	2002-11-08	1	F160W
Pointed Flat	n8um01	2003-10-15	1	F160W
Pointed Flat	n8um04	2004-04-25	1	F160W
Pointed Flat	n94n02	2005-03-31	1	F160W
Pointed Flat	n9hy01	2005-10-28	1	F160W
Pointed Flat	n9vf01	2006-11-07	1	F160W
Pointed Flat	n9vf02	2007-01-21	1	F160W
Pointed Flat	n9vf03	2007-02-07	1	F110W
Pointed Flat	n9hy01	2006-02-13	2	F160M
Pointed Flat	n9vf02	2007-01-21	3	F160W
Pointed Flat	n9hy02	2006-02-13	3	F160W
Pointed Flat	n9vf04	2007-08-26	2	F222M
NGC 3603	n9voa1	2007-01-20	1	F090M
NGC 3603	n9vo01	2007-01-20	1	F110W
NGC 3603	n9vo01	2007-01-20	1	F160W
NGC 3603	n9voa4	2006-11-28	2	F110W
NGC 3603	n9vo01	2007-01-20	2	F160W
NGC 3603	n9vo05	2006-11-28	3	F110W
NGC 3603	n9vo04	2006-11-28	3	F150W

All cluster observations were reduced using the standard calnica pipeline, except the dark frames which were only reduced through the ZSIGCORR and the ZOFFCORR calibration steps. Both the _ima and _cal data products were used for this analysis. All _ima

files for each camera and filter combination, taken before the flat field lamp was used, were averaged together with MSCOMBINE. Similarly, all corresponding _cal files were averaged together. All the lamp-on images for a unique camera, filter combination were averaged as well. Lamp-off images taken after the flat field lamp-on images, were not used since they contain count persistence from the lamp-on observations. The small number of lamp-off images due to this restriction, limits the possible S/N that was attainable with these data sets. Despite averaging, both noise and changing bias levels limits our investigation to a count range greater than 100 ADU. In this range, the noise has been sufficiently constrained and the non-linearity tests produce useful results. To test the non-linearity for counts below 100 ADU, more lamp off data sets are needed, as well as longer exposures. However, for the purposes of this investigation, using only counts that are greater than 100 ADU will suffice to show that at moderate to high count levels the NICMOS count non-linearity has been corrected to within a few percentage of true linearity

The final averaged _ima files were converted to counts by multiplying each extension by the samptime keyword. Dependence on previous readouts were removed by using SAMPDIFF to subtract the previous readout from each extension. The resultant images were then converted back into count rates by dividing by the deltatime keyword for each extension. Data quality masks were applied to remove all flagged pixels except those containing signal in the 0th read since all the pixels in the lamp-on images would be unnecessarily flagged. All pixels in the _cal files were logarithmically binned by count rate, and these pixel bins were subsequently used to investigate the average count rate in the different samples of the _ima files. Figure 1 shows the individual readouts for the final products from SAMPDIFF in units of count rate for a NIC1 lamp on set. The following color coded data quality flags are overlaid on the image:

Table 2. Data quality flags and corresponding colors used in Figures one and two.

Data Quality Flag	Color
Reed Solomon	Cyan
Bad Linearity Correction	Magenta
Bad Flat Field Correction	Maroon
Bad Back-ground Sub-traction	Orange
Defective Pixel	Blue
Saturated Pixel	Green
Missing Data	Khaki
Bad Pixel Detected by Calibration	Red
Cosmic Ray	Yellow

Figure 1: Multiaccum readouts output from sampdiff in count rates of NGC 3603 with flat field lamp for NIC 1, F160W, samp_seq =STEP16, exposure time~ 80 seconds. Images are ordered from first readout to last going left to right with overlaid data quality flags.

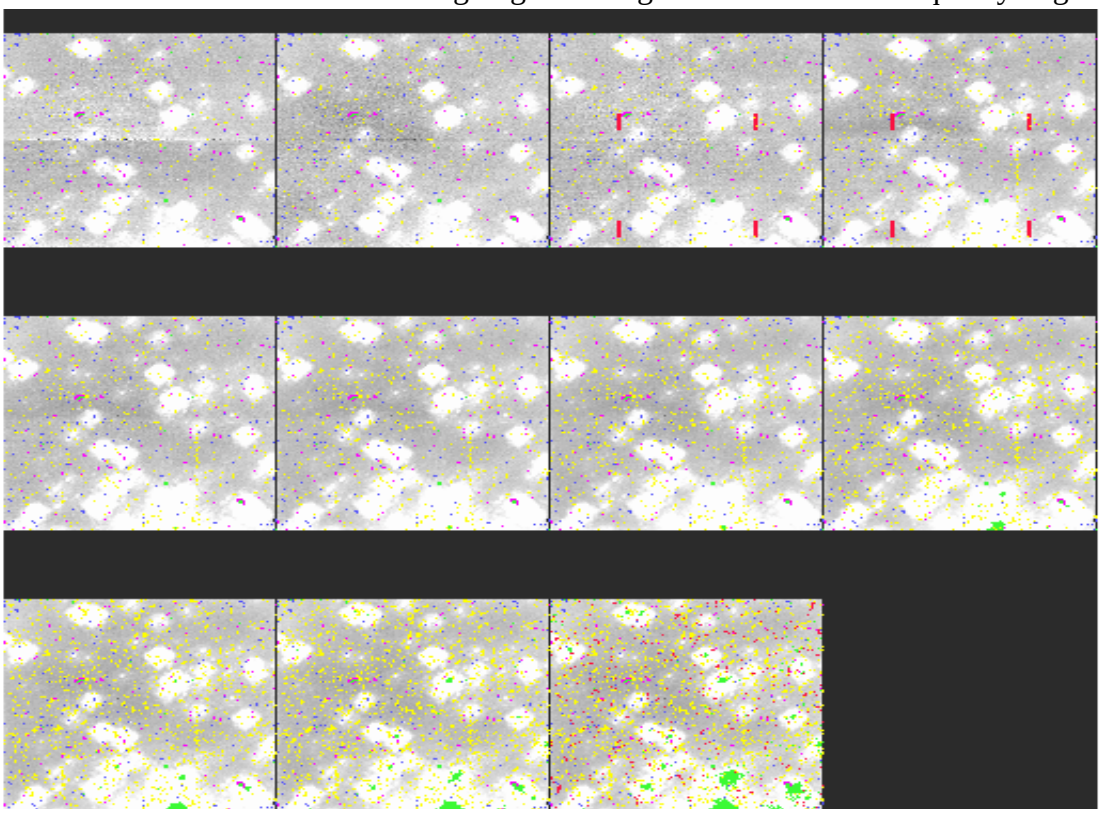

The pointed flat observations were also reduced using the standard calnica pipeline. However, the lamp-off images were used as darks and prepared by using only the ZSIG-CORR and ZOFFCORR steps in calnica. They were then median combined and used as the DARKFILE for processing the lamp on images through the full calnica pipeline. The final _ima and _cal lamp on images were each median combined and used for further processing. As with the cluster data the _ima file were converted to counts using the samptime keyword. The subsequent readouts subtracted from one another with SAMP-DIFF and converted back into count/s with the deltatim keyword. Data quality masks were applied to remove all flagged pixels except those containing signal in the 0th read. The individual readouts of the final products for one of the datasets is shown in Figure 2.

Figure 2: Pointed flat field readouts from sampdiff output in count rates for camera 1, filter F160W, samp_seq =STEP8, exposure time~152 seconds. Images are ordered from first readout to last going left to right with overlaid data quality flags.

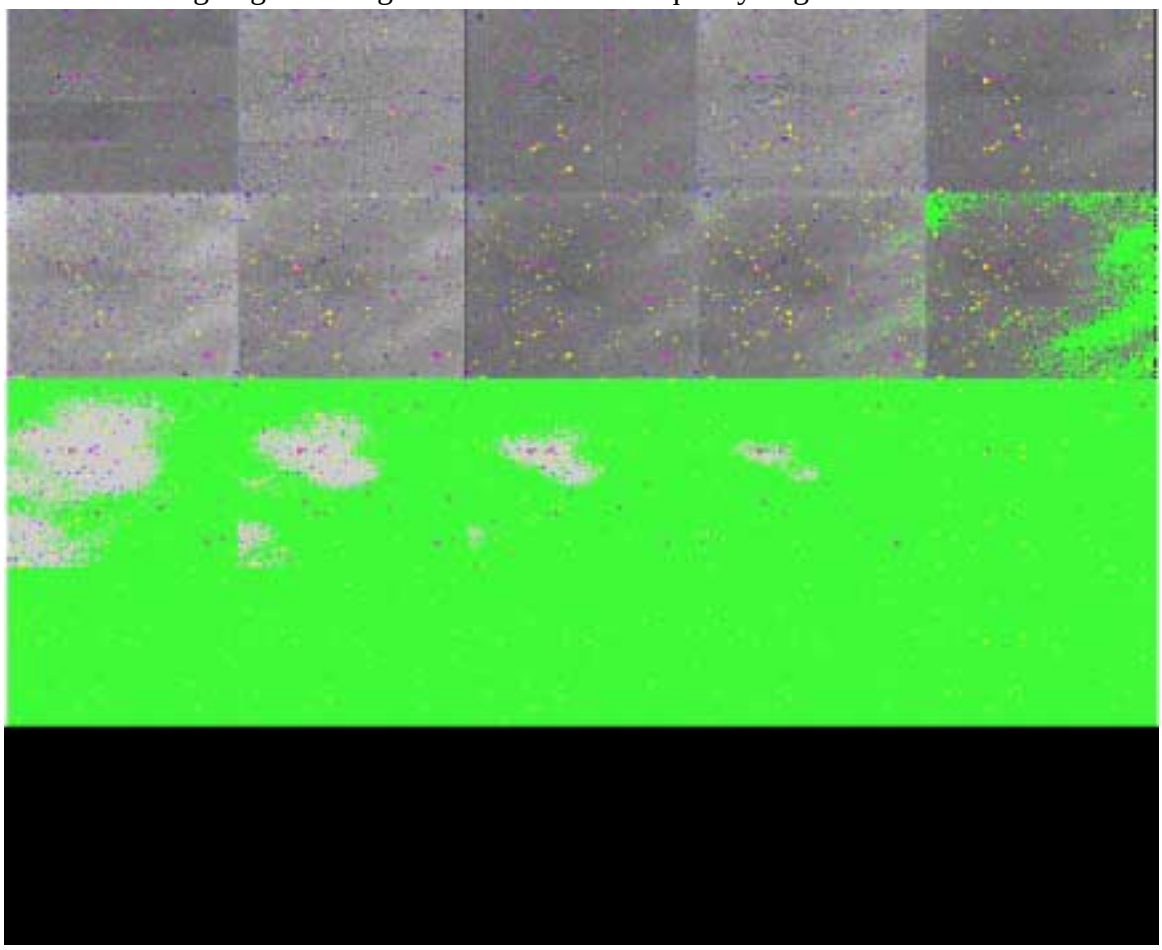

Results

To test the linearity correction, we look at the countrate of a pixel as function of the counts in the pixel. Figures 3-6 show the average of a count rate bin in the _ima files normalized to the average of the same bin in the _cal files as a function of average counts in

the _ima bin. For all lamp-off images the average value for the smallest count rate bins were subtracted from all other bin averages to minimize fluctuations in the counts due to bias jumps. Error in the average count rate for an individual bin is represented as the inverse square root of the number of contributing pixels. Error bars are not included in the lamp-off plots to keep them legible, especially near the 100 count range.

Figure 3: Count non-linearity test for lamp off cluster images.

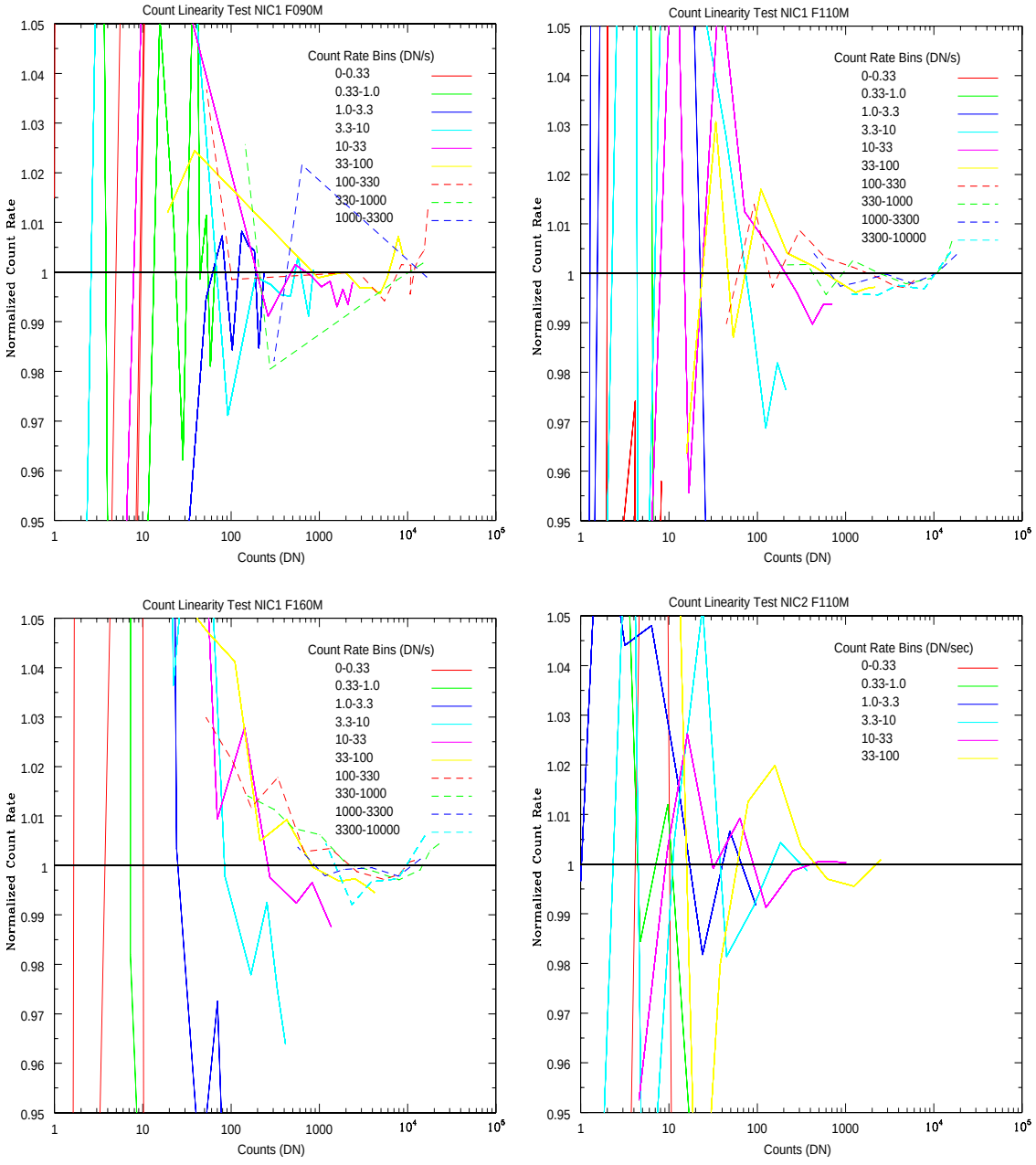

Figure 4: Count non-linearity test for lamp off cluster images.

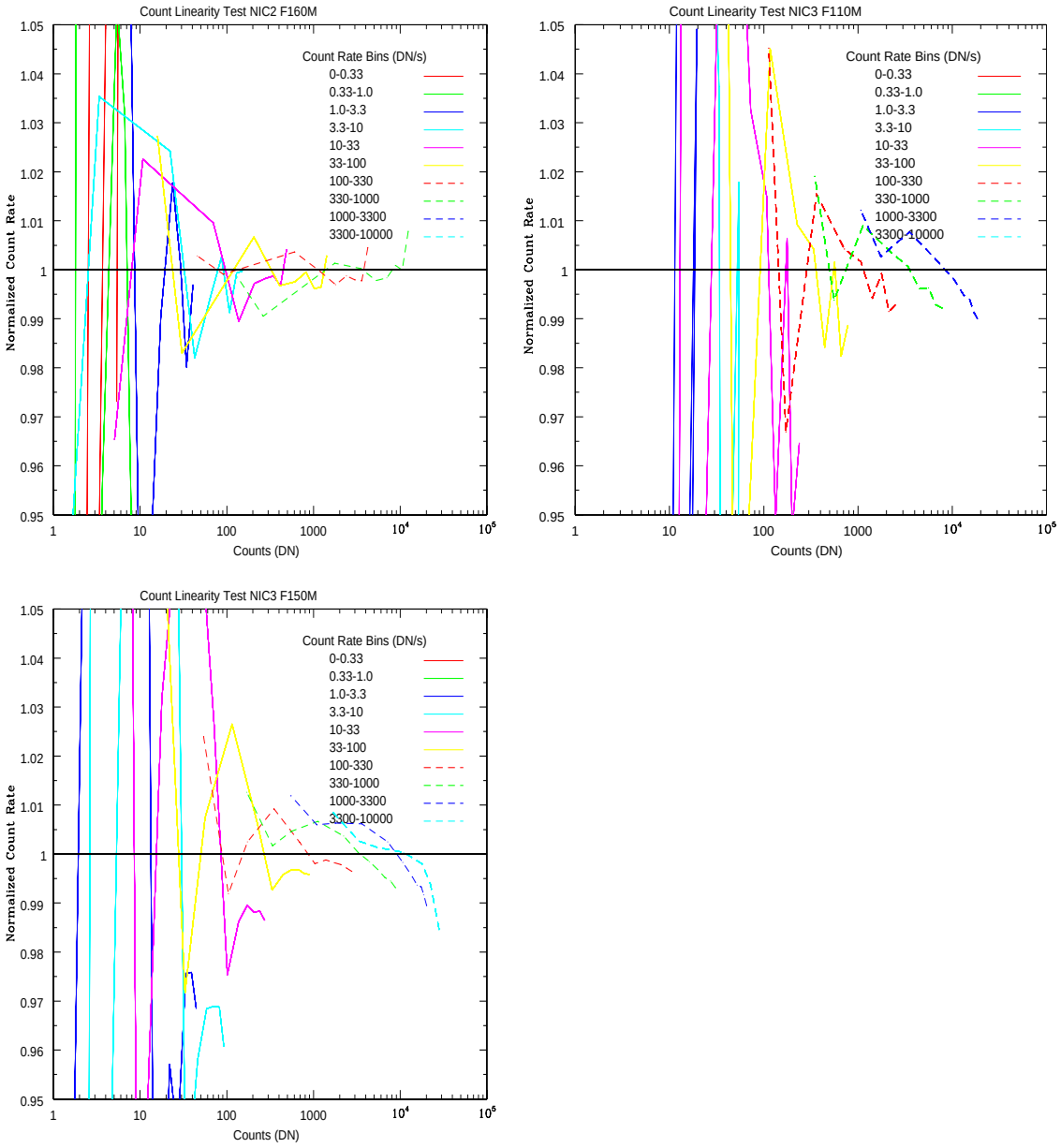

Figure 5: Count non-linearity test for lamp on cluster images.

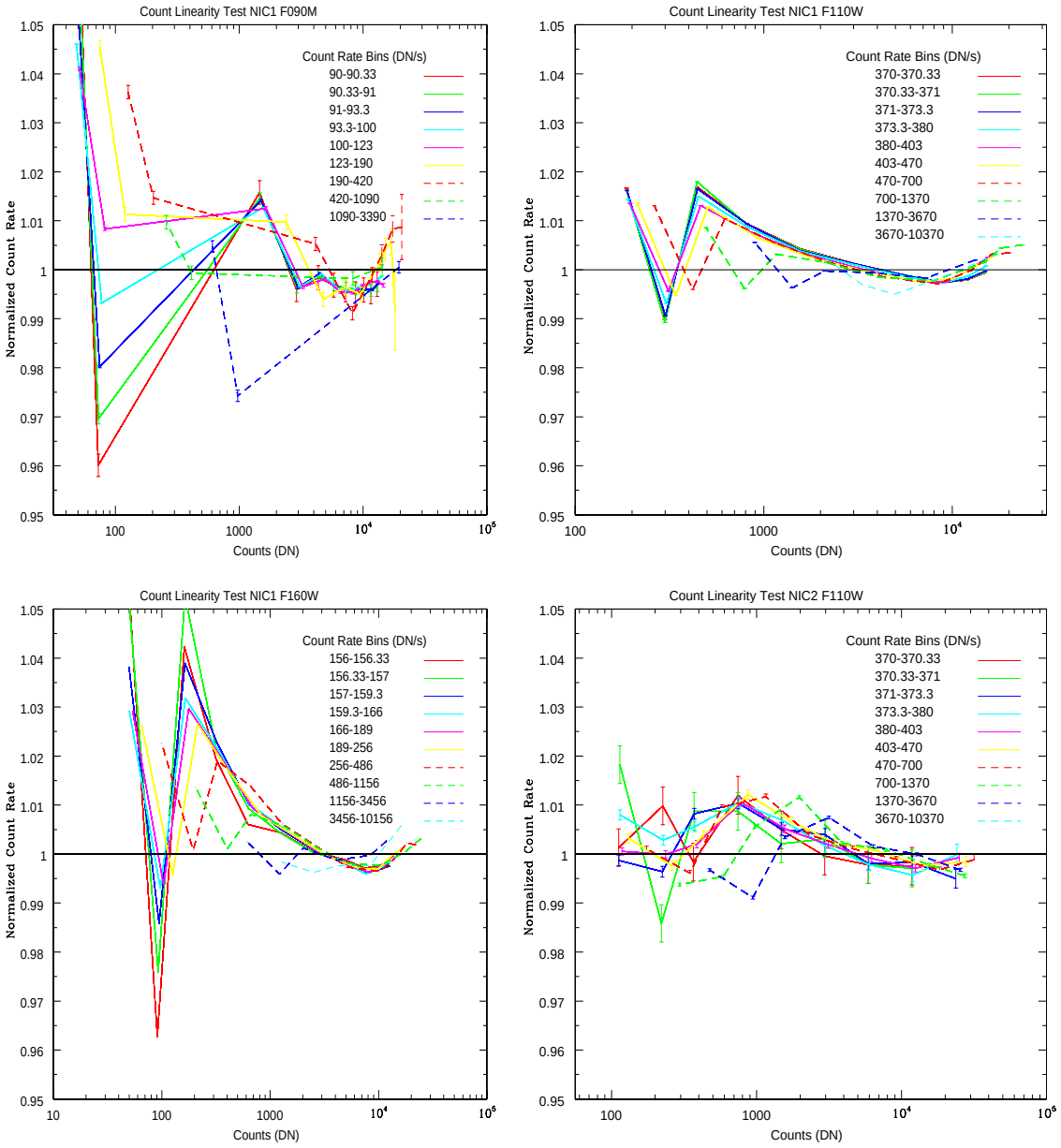

Figure 6: Count non-linearity test for lamp on cluster images.

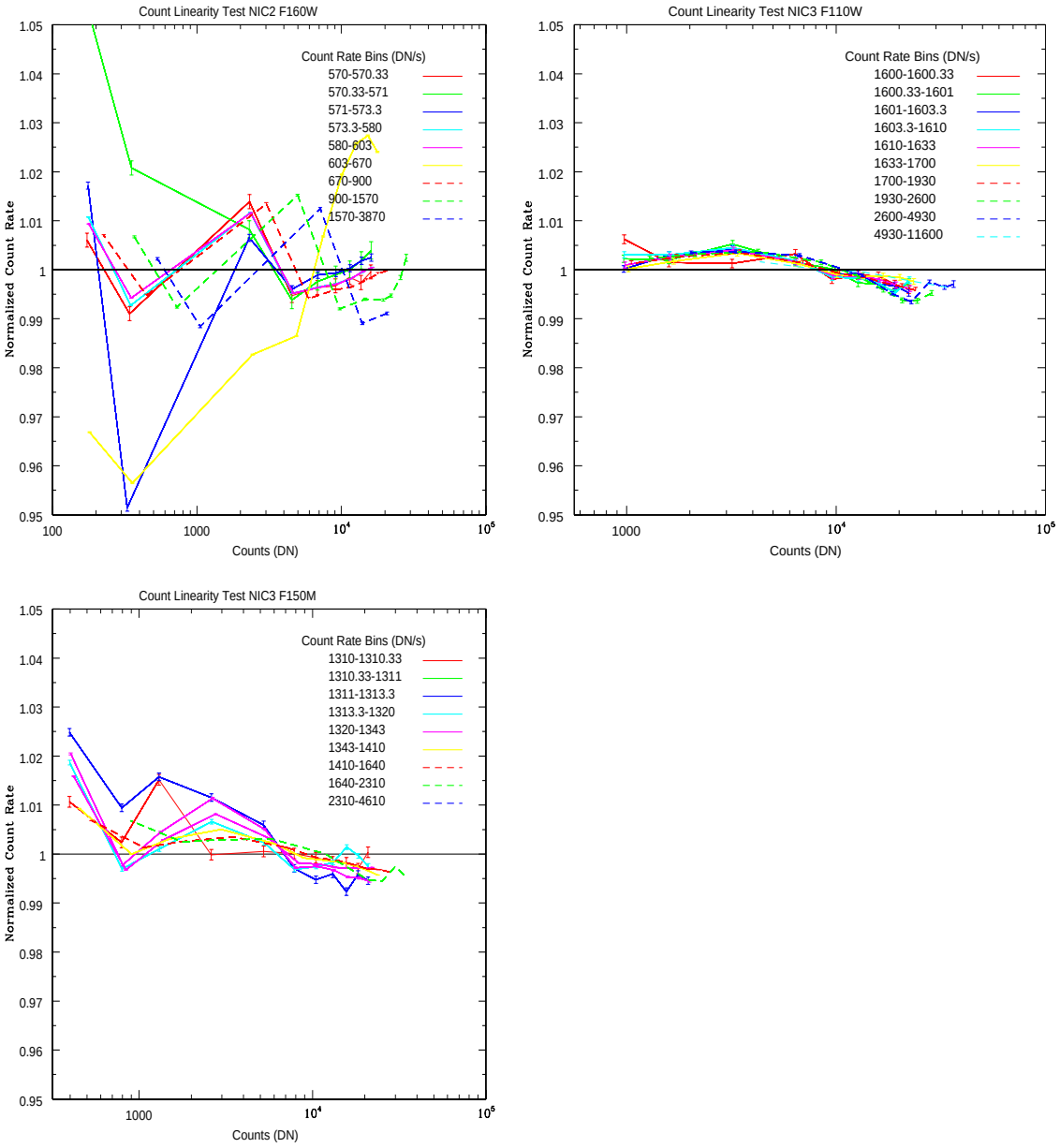

A similar test was performed on the pointed flats and one of the cluster images. Instead of binning, thirty random pixels for each quadrant of the images were chosen. The count rate of these pixels in the sampdiff output was normalized to the count rate in the _cal file and plotted versus the counts in the sampdiff output for each readout. Below each plot is the average of all the pixels in the quadrant for each readout with errors bars indicating one standard deviation of the count rate, unless otherwise indicated. Quadrants are labeled as a-d clockwise around the image starting in the upper left corner. To verify that there are

no undetected saturation in the pixels, the counts of the same random pixels are plotted versus time in Figures 8,10, and 12.

Figure 7: Count Linearity Test for 30 random pixels in each quadrant of a NGC 3606 image with the flat field lamp for NIC 1, filter F160W. Below each linearity test is the average behavior for the entire quadrant with one standard deviation of the count rate.

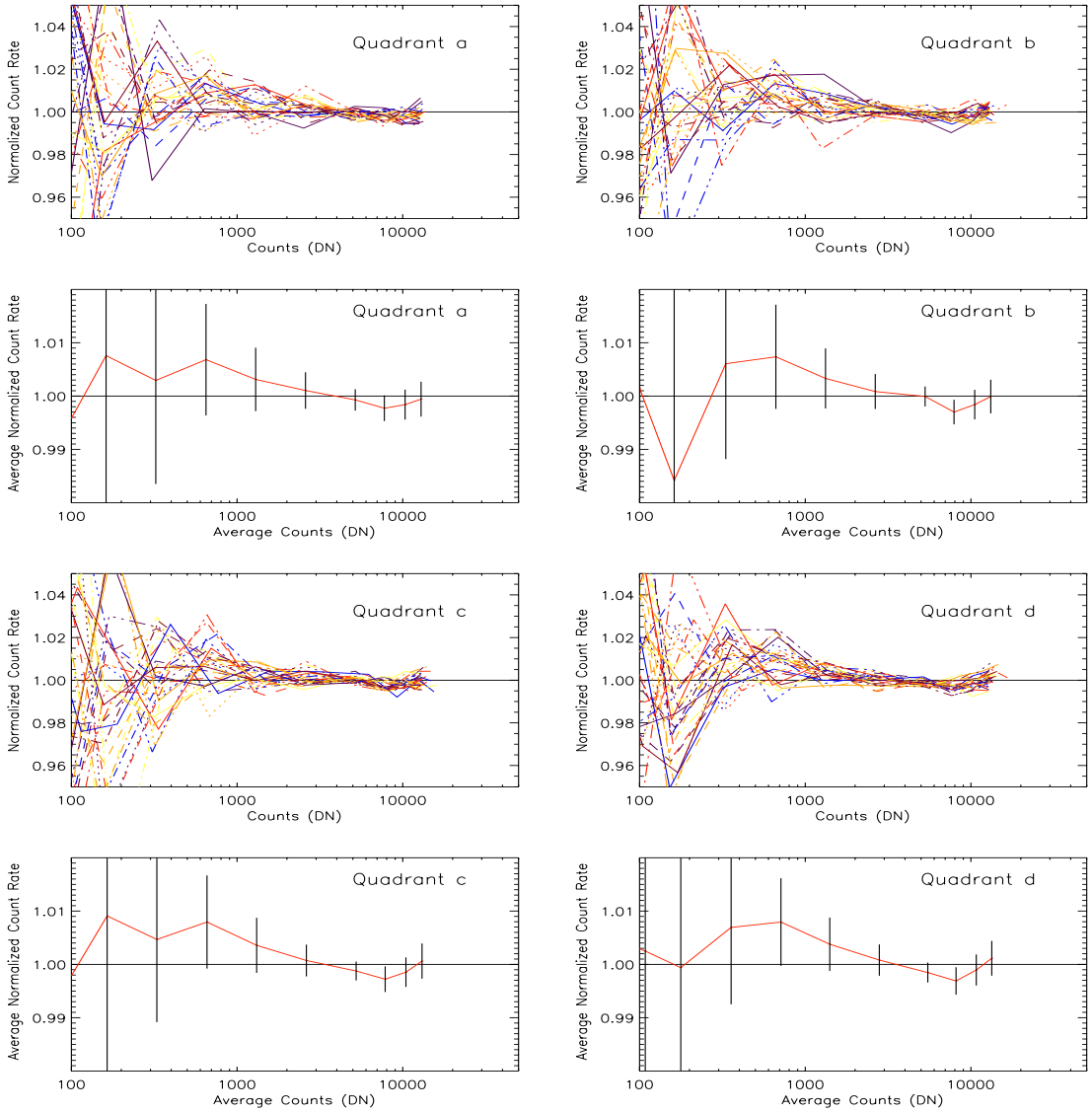

Figure 8: Counts versus time for same images and pixels used to create Figure 7. The plots in red show the actual pixels used for the linearity test, while the plots in blue show the same pixels without using data quality information to throw out bad pixels.

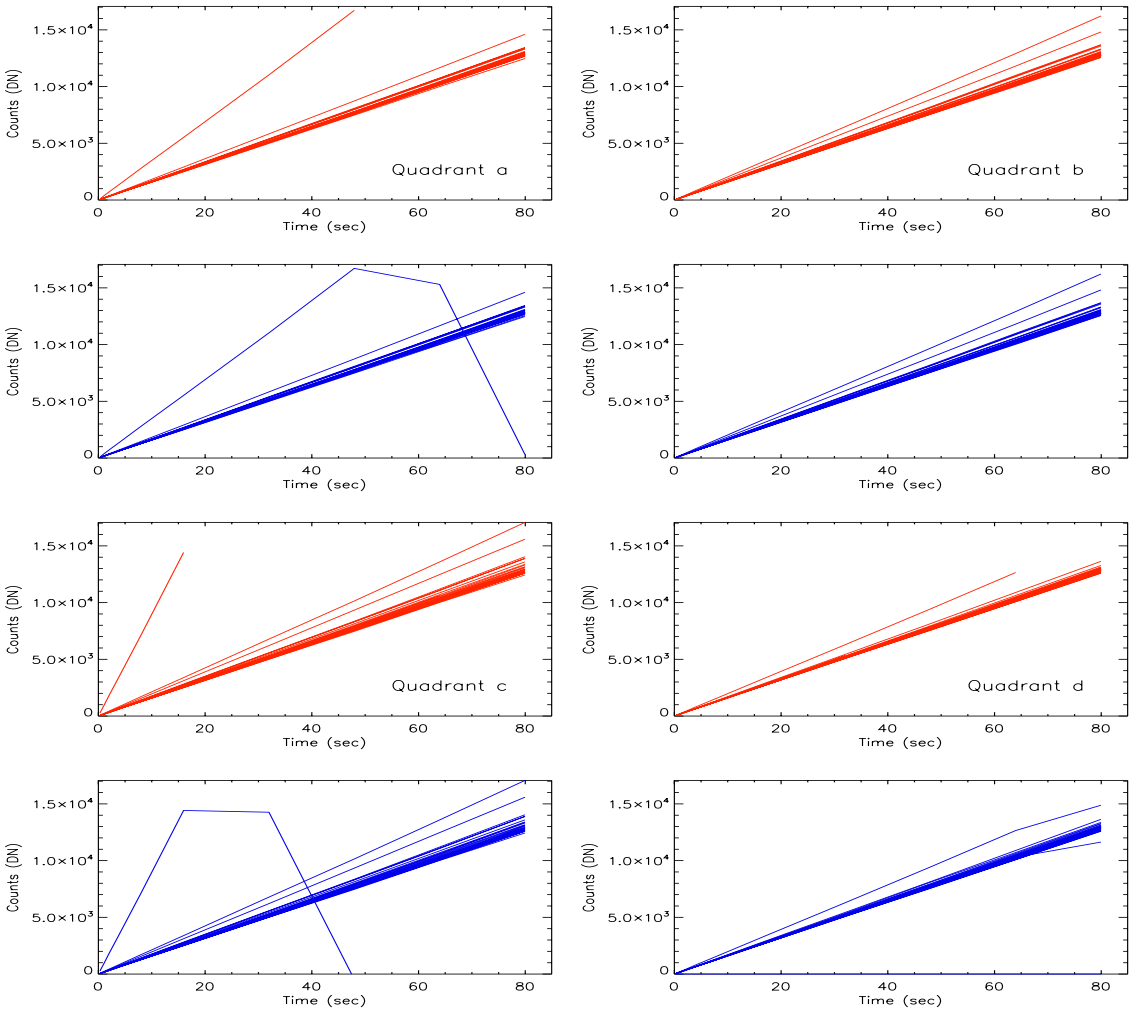

Figure 9: Count Linearity Test for 30 random pixels in a pointed flat field (previously shown in figures 2) for NIC 1, filter F160W. Below each linearity test is the average behavior for the entire quadrant with one standard deviation of the count rate .

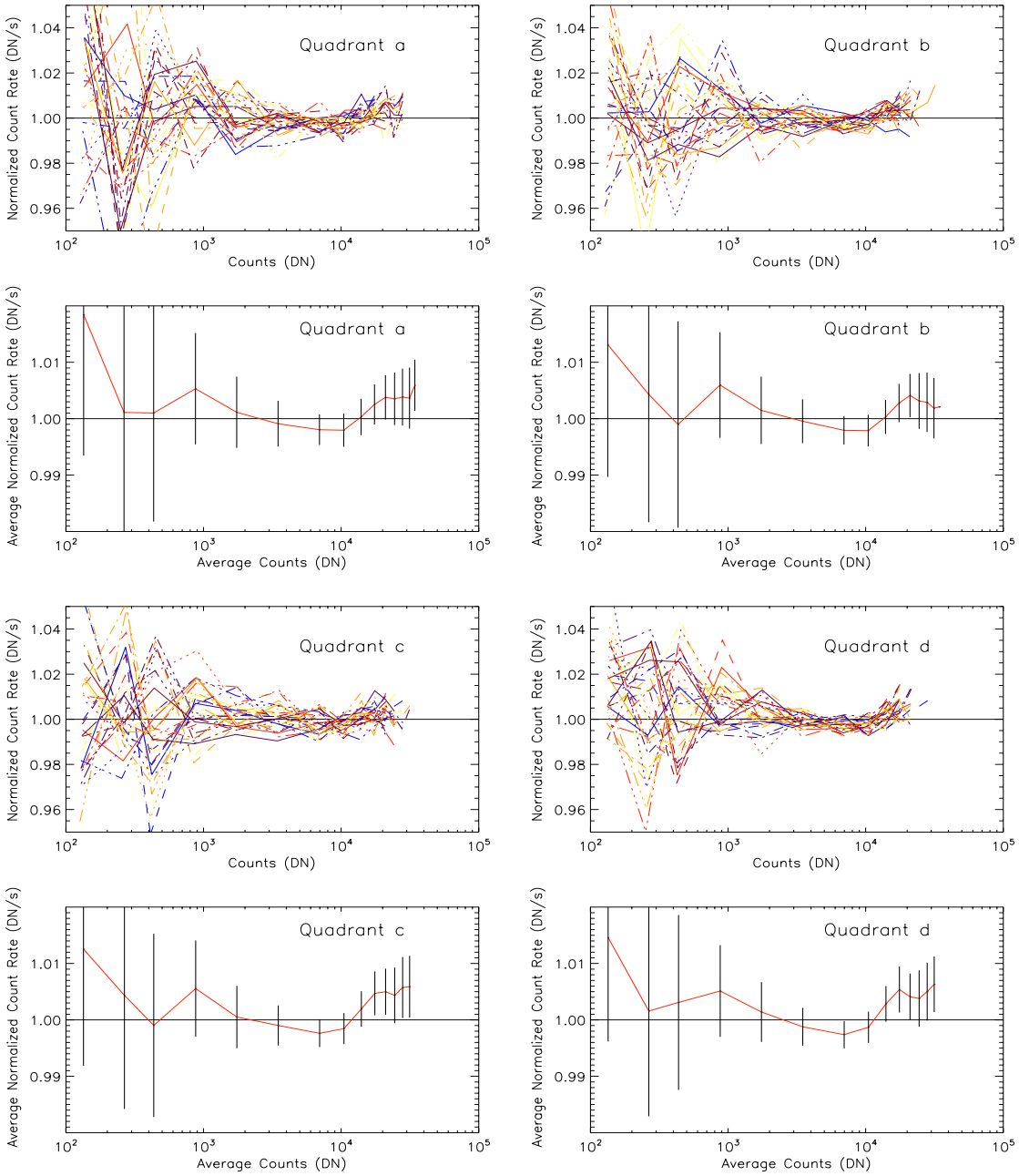

Figure 10: Counts versus time for same images and pixels used to create Figure 10. The plots in red show the actual pixels used for the linearity test, while the plots in blue show the same pixels without using data quality information to throw out bad pixels. Notice there are no grossly saturated pixels used in the linearity test, even though there is clear saturation in some of the pixels for longer readouts.

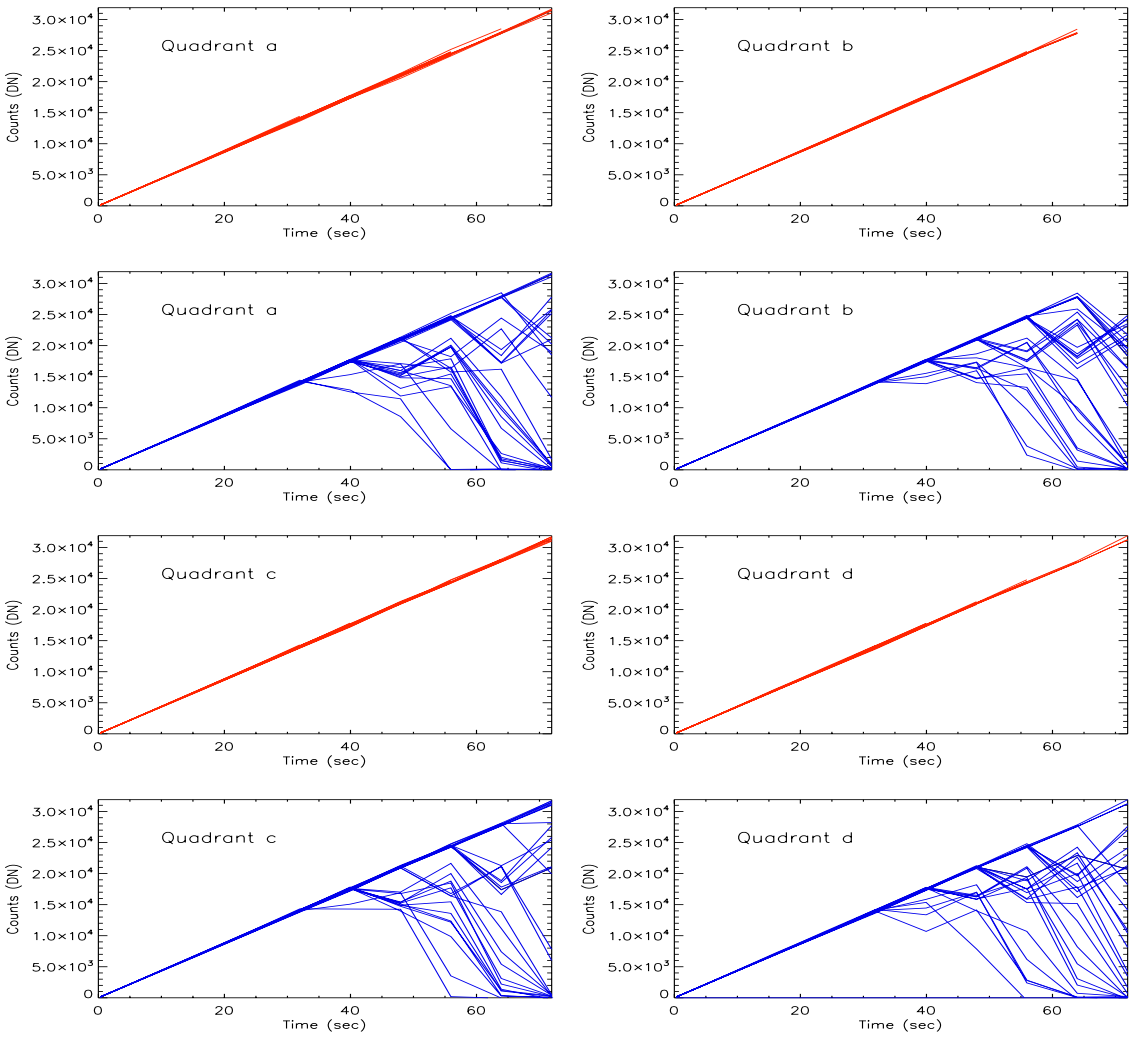

Figure 11: Count Linearity Test for 30 random pixels in a pointed flat field for NIC 1, filter F110W. Below each linearity test is the average behavior for the entire quadrant with one standard deviation of the count rate .

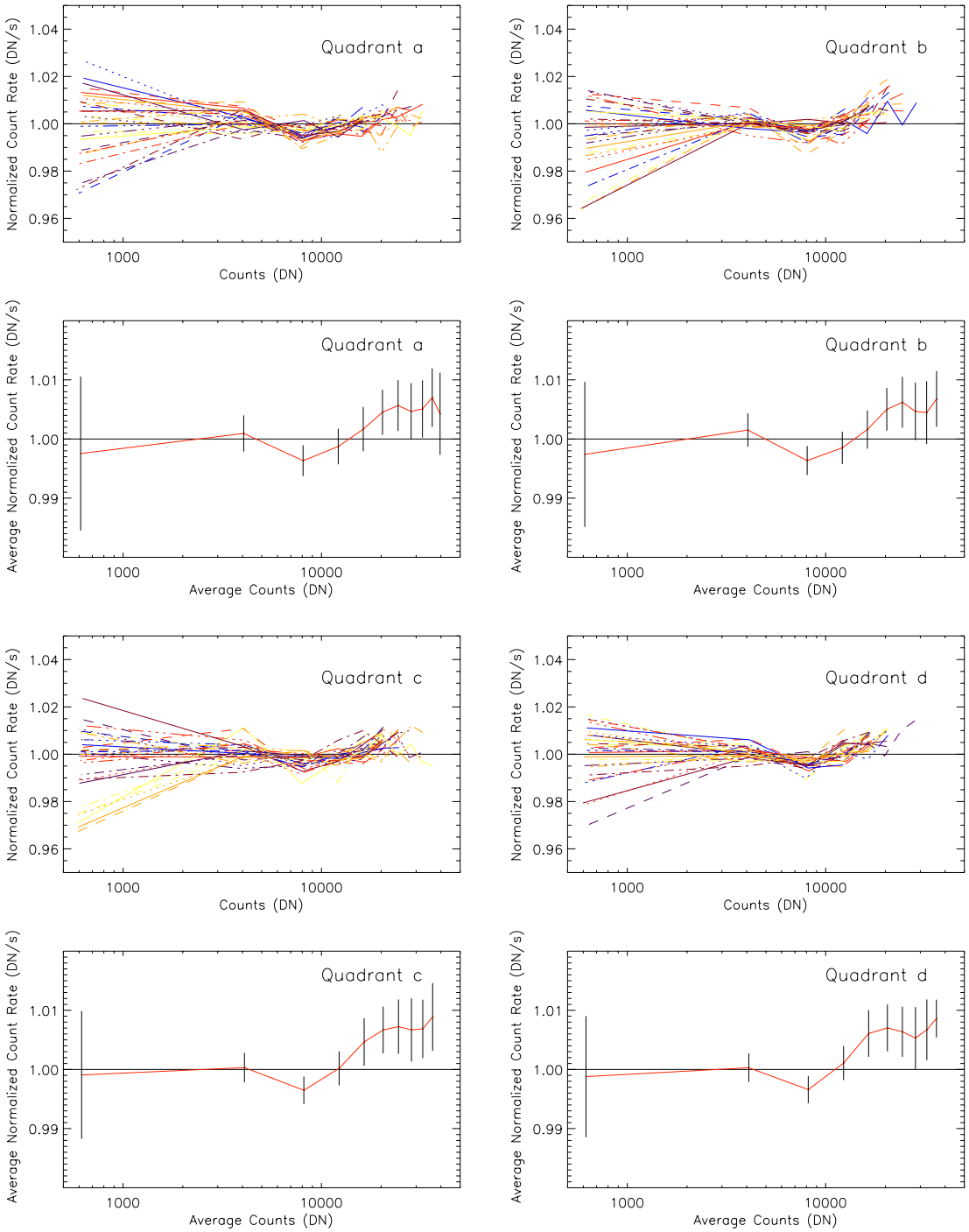

Figure 12: Counts versus time for same images and pixels used to create Figure 11. The plots in red show the actual pixels used for the linearity test, while the plots in blue show the same pixels without using data quality information to throw out bad pixels.

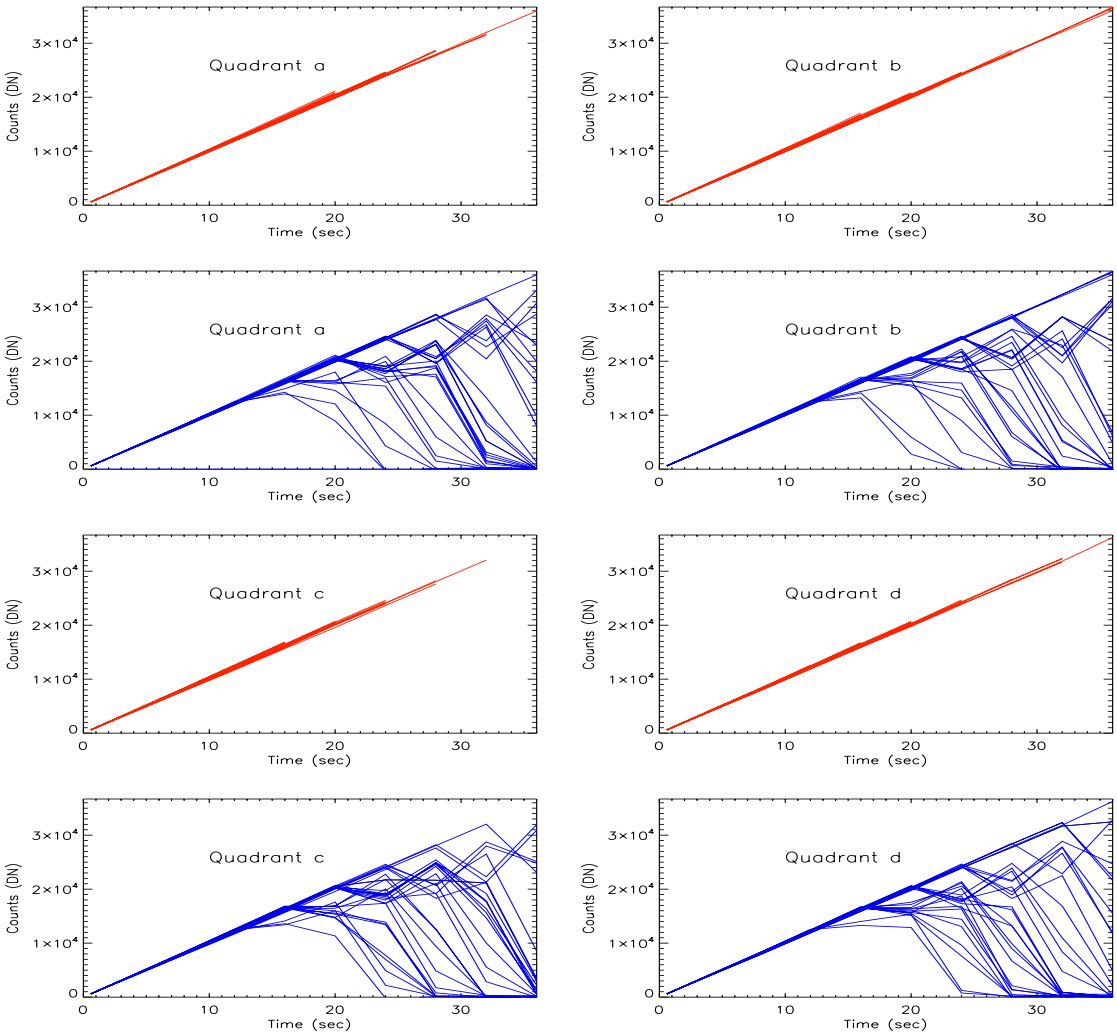

Figure 13: Count Linearity Test for 30 random pixels in each quadrant of a pointed flat for NIC 2, filter F160W. Below each linearity test is the average behavior for the entire quadrant with two standard deviations about the mean.

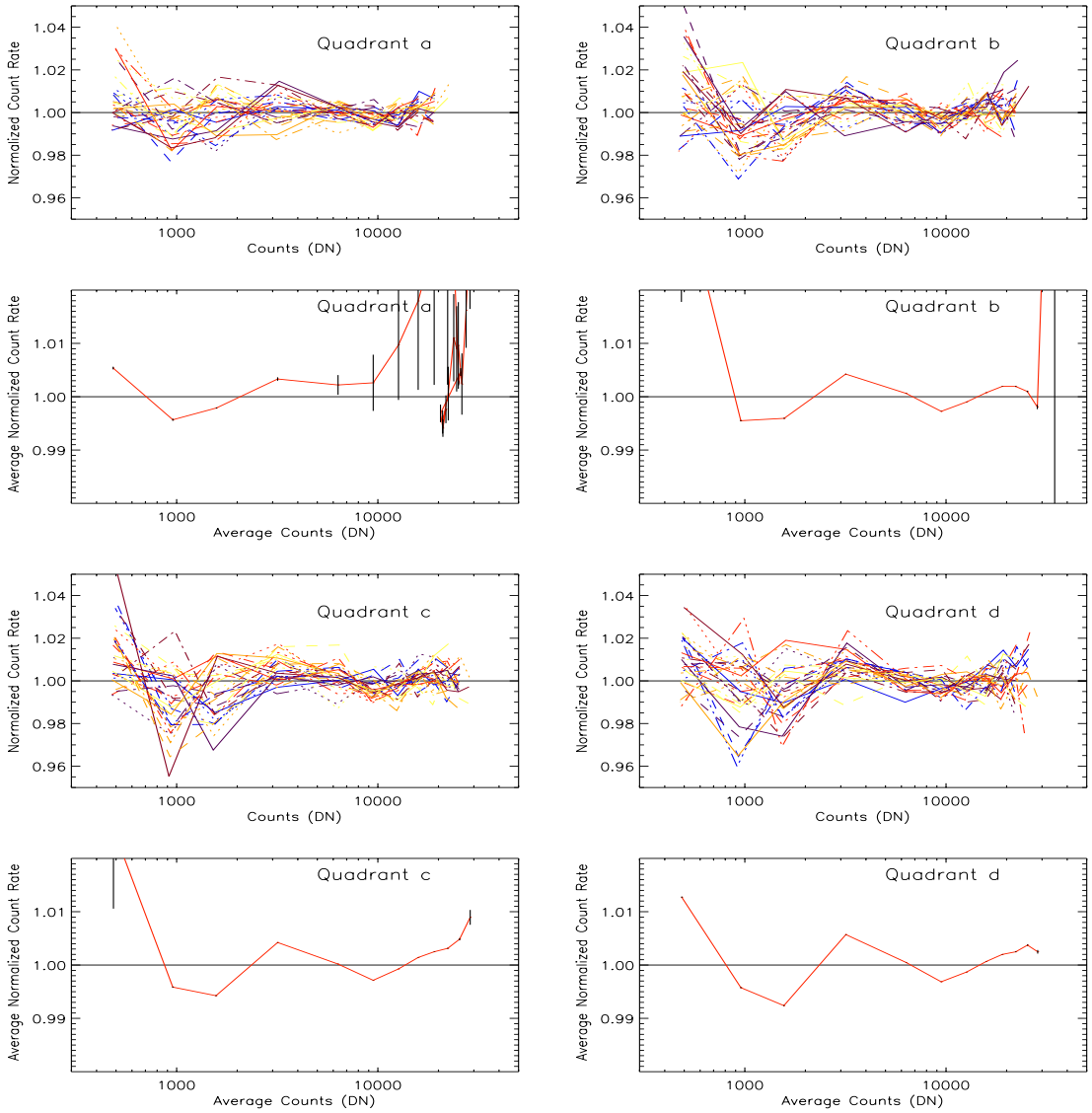

Figure 14: Count Linearity Test for 30 random pixels in each quadrant of a pointed flat for NIC 2, filter F222M. Below each linearity test is the average behavior for the entire quadrant with two standard deviations about the mean

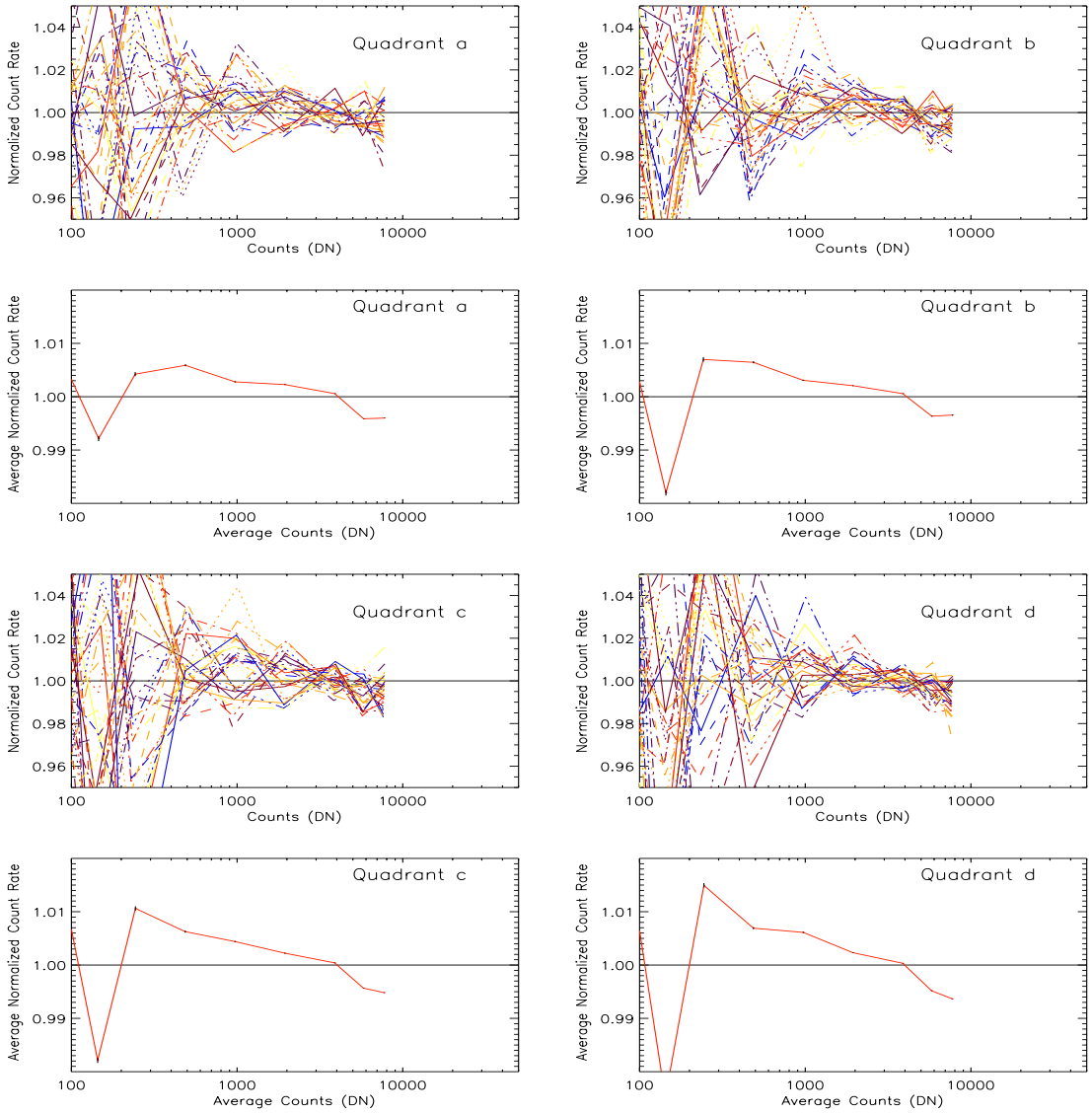

Figure 15: Count Linearity Test for 30 random pixels in each quadrant of a pointed flat for NIC 3, filter F160W taken in 2006. Below each linearity test is the average behavior for the entire quadrant with two standard deviations about the mean.

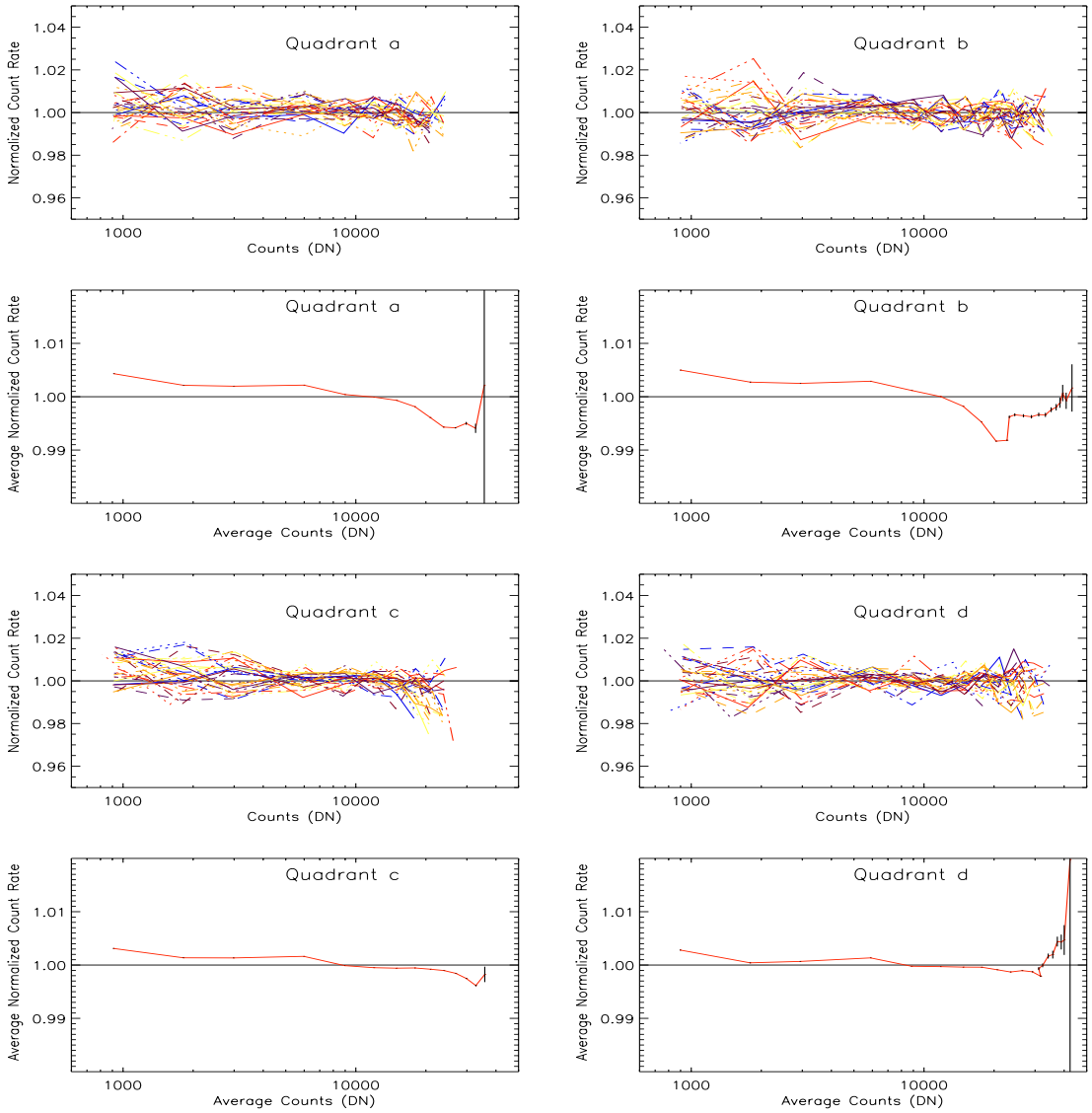

Figure 16: Count Linearity Test for 30 random pixels in each quadrant of a pointed flat for NIC 3, filter F160W taken in 2007. Below each linearity test is the average behavior for the entire quadrant with two standard deviations about the mean

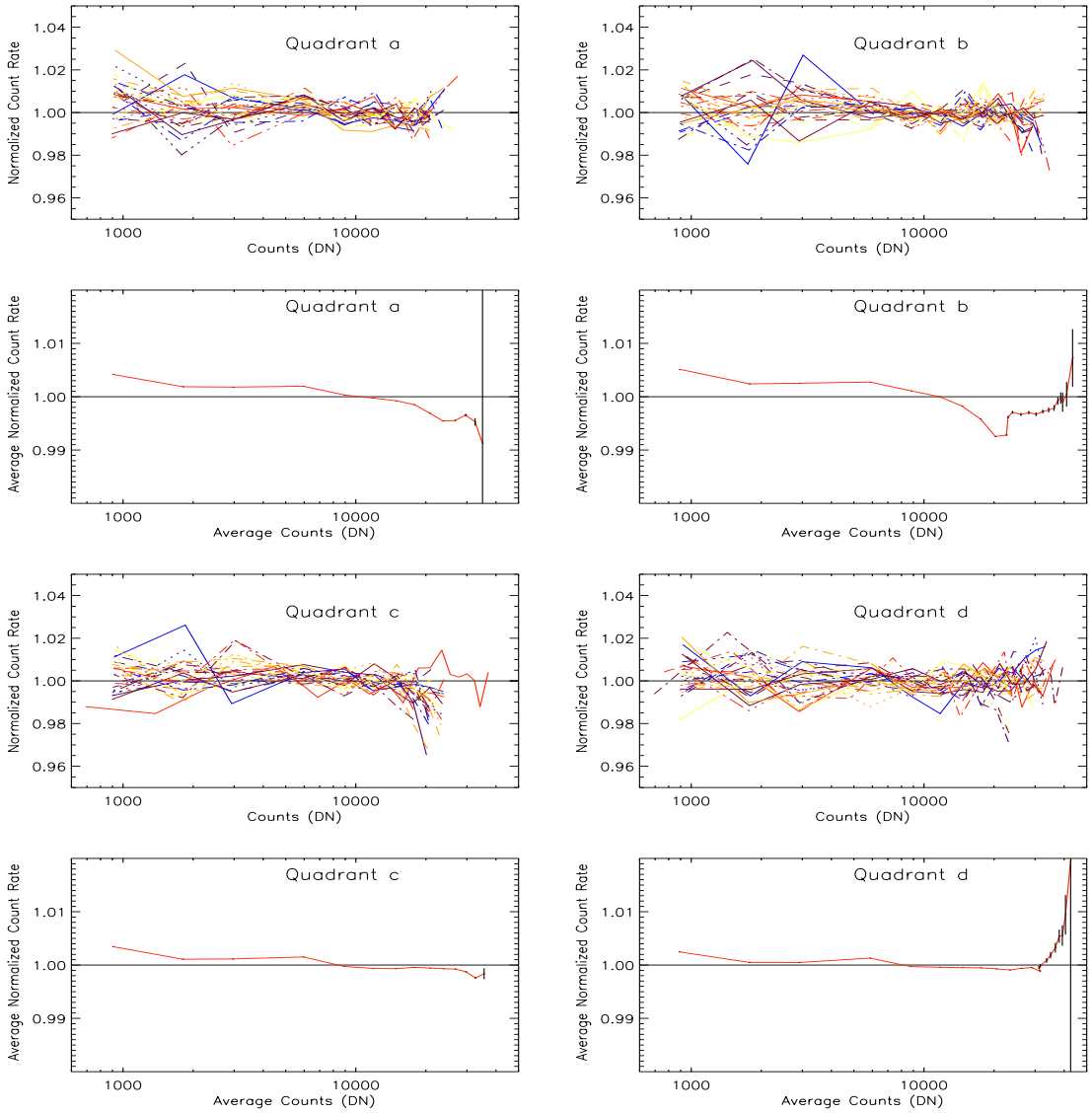

Analysis

On first analysis, it appears the count correction improves with higher counts. This is likely just the improvement in signal-to-noise for longer exposure times. The NIC 1, cluster plots show a slight non-linearity from +1% to ~ -0.5% between 100 and 5000 ADU. Above 5000 ADU the non-linearity increases again to ~+1%. The pointed flat field data verifies that NIC 1 does indeed appear to have a similar non-linearity as seen in the cluster

data. The normalized count rate in the pointed flats decreases to -0.3% at 5000 counts then increases to +~1% for greater counts. Additionally, all quadrants in this camera exhibit this behavior consistently over the course of a few years for both Pre-NCS and Post-NCS data regardless of the filter used. Appendix A includes linearity plots from pointed flats taken with NIC 1 and filter F160W from 1997 to 2006. We recommend re-deriving the count non-linearity parameters for NIC 1.

The NIC 2 results are more difficult to characterize. There does not seem to be any systematic offset in the correction, but rather a random distribution about unity. The NIC 3 plots shows a systematic decrease in count rate, but it seems to be more related to time than to total counts. The cause of this effect is currently not clear.

Conclusions

The overall trend for all filters and cameras is a maximum median offset of no more than 1.24% for counts above 100 ADU. The count dependent non-linearity correction appears to still be accurate for both NIC 2 and NIC 3 cameras. The slight non-linearity in the NIC 1 results should be further investigated and corrected for counts above 100 ADU.

References

Barker, E., Pirzkal, N., et al. 2006, "NICMOS Instrument Handbook", Version 9.0, (Baltimore: STScI)

Appendix A

This appendix includes plots of linearity tests for NIC1 1 with filter F160W data taken from 1997 to 2006.

Figure 17: Count Linearity Test for 30 random pixels in each quadrant of a pointed flat field image taken in 1997 for NIC 1, filter F160W. Below each linearity test is the average behavior for the entire quadrant with 2 sigma about the mean. Note this data was taken before the installation of NCS.

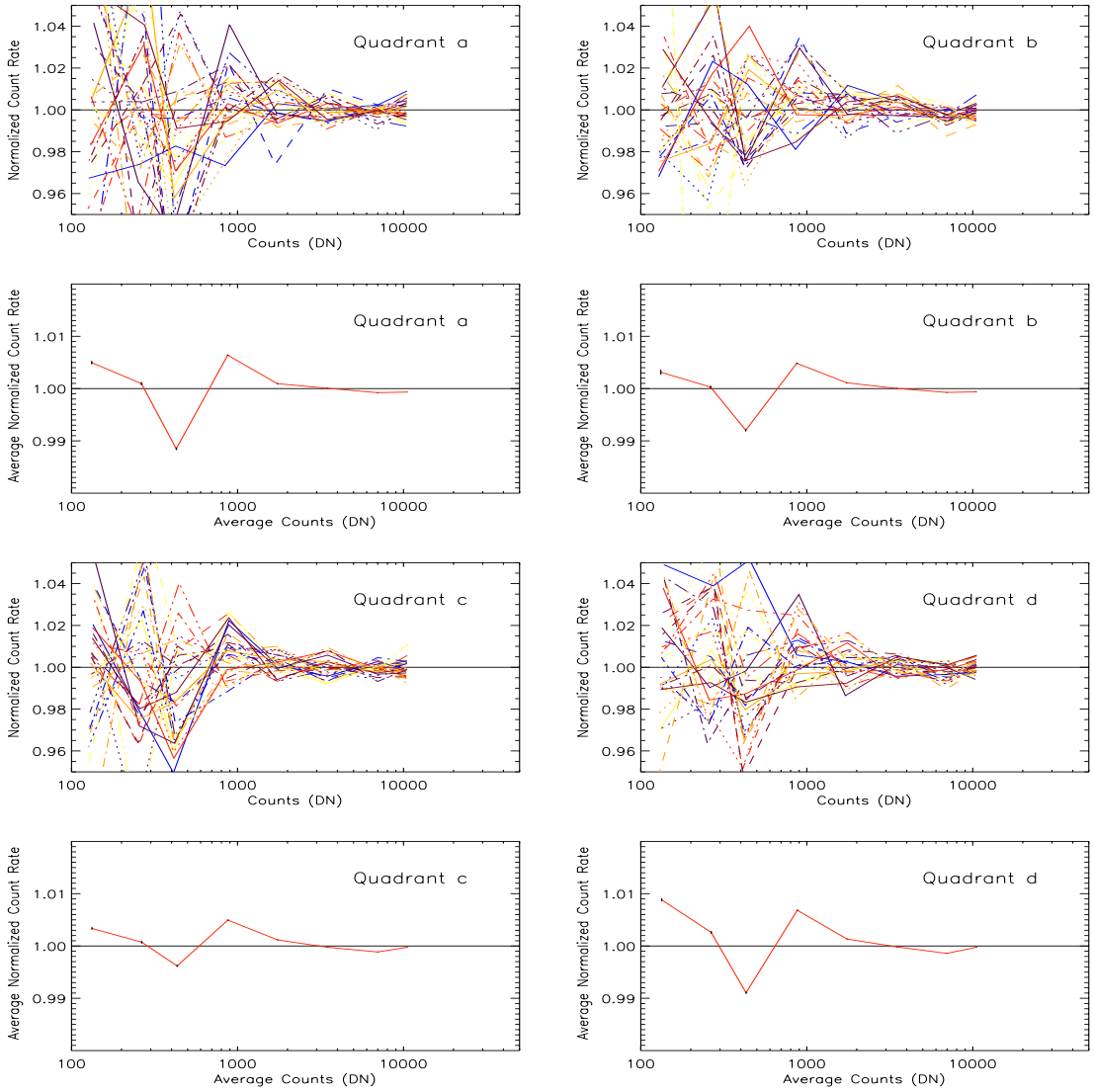

Figure 18: Count Linearity Test for 30 random pixels in each quadrant of a pointed flat field image taken in July 2002 for NIC 1, filter F160W. Below each linearity test is the average behavior for the entire quadrant.

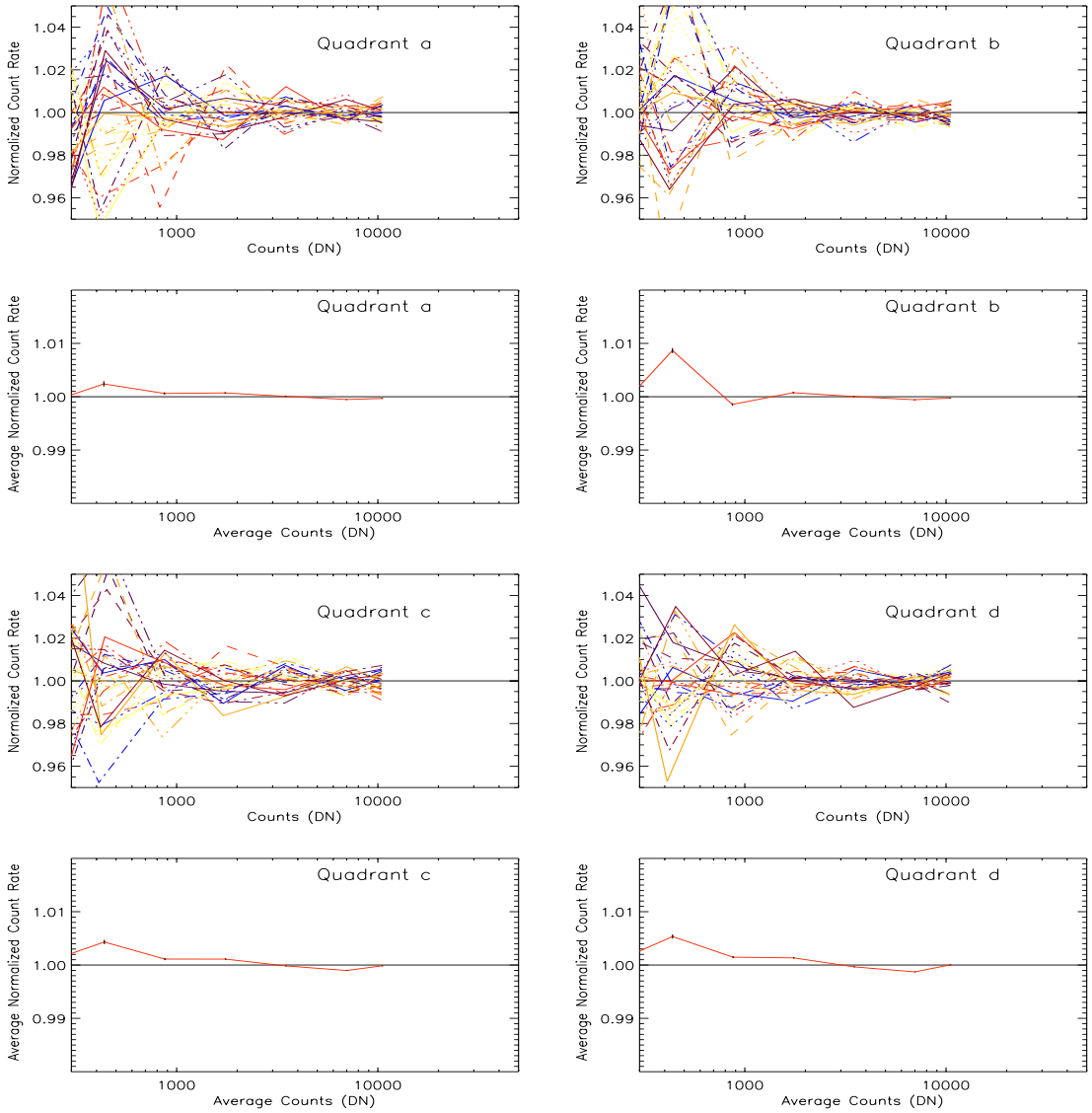

Figure 19: Count Linearity Test for 30 random pixels in each quadrant of a pointed flat field image taken in November 2002 for NIC 1, filter F160W. Below each linearity test is the average behavior for the entire quadrant with 2 sigma about the mean.

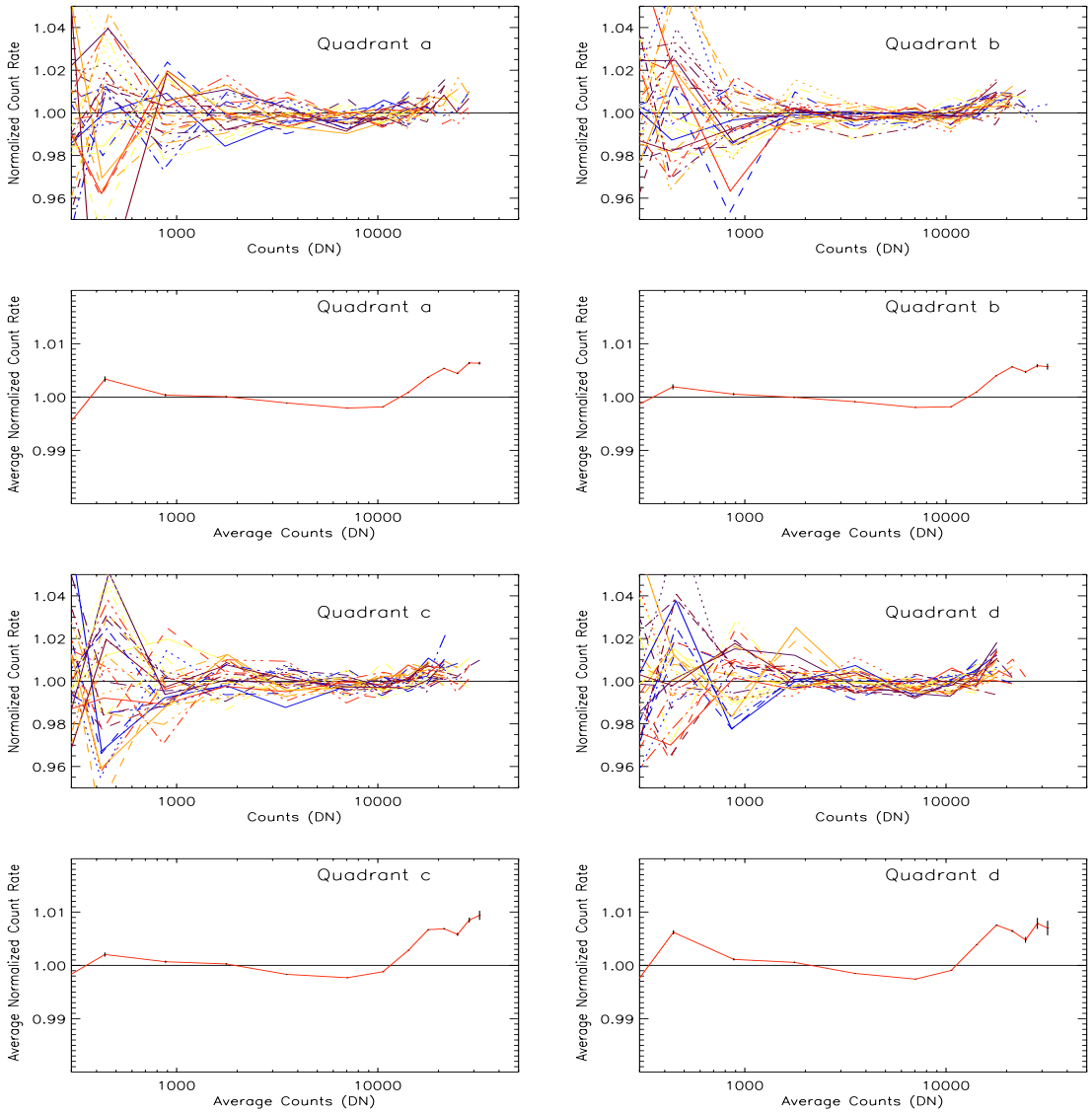

Figure 20: Count Linearity Test for 30 random pixels in each quadrant of a pointed flat field image taken in October 2003 for NIC 1, filter F160W. Below each linearity test is the average behavior for the entire quadrant with 2 sigma about the mean.

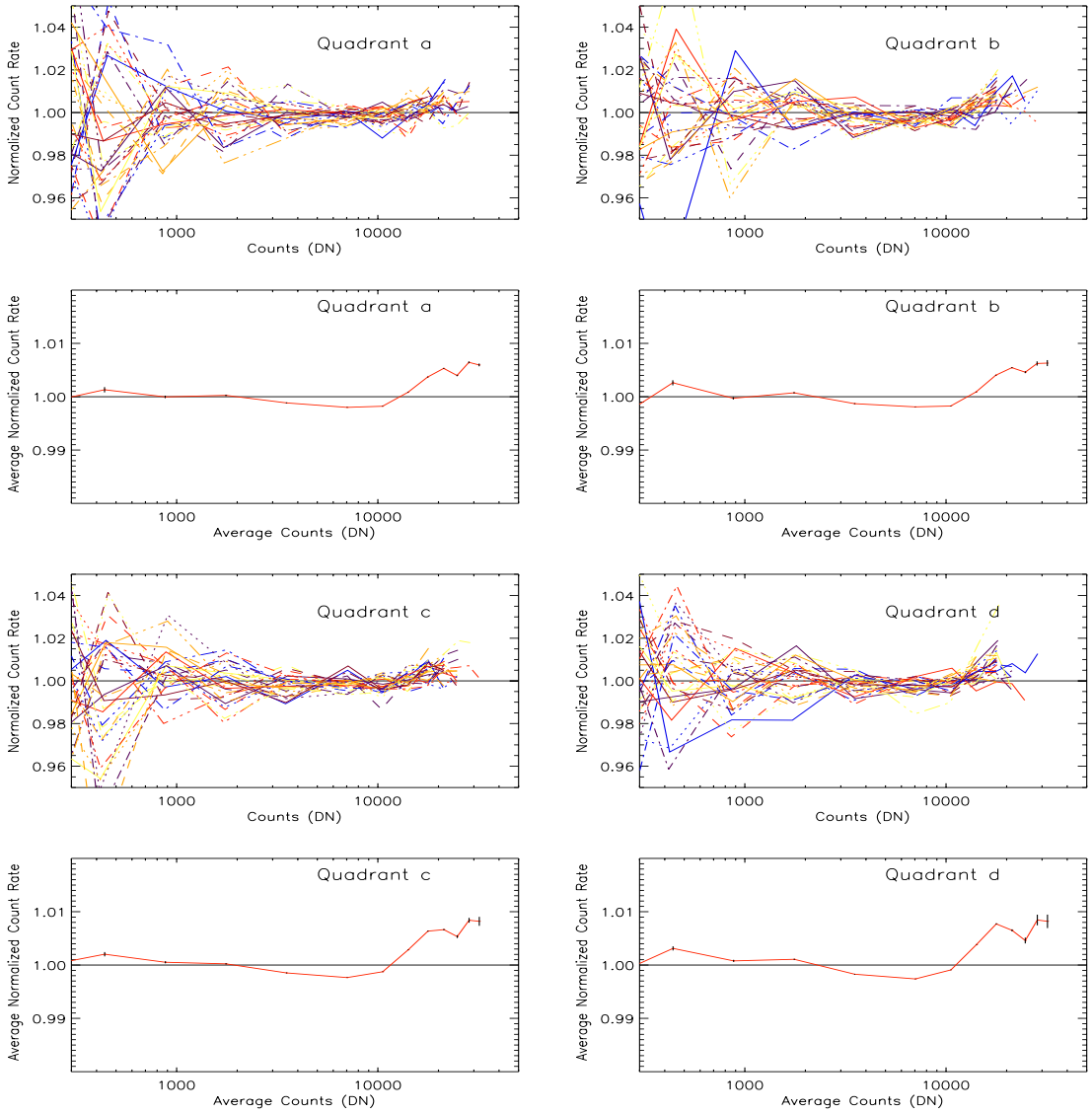

Figure 21: Count Linearity Test for 30 random pixels in each quadrant of a pointed flat field image taken in April 2004 for NIC 1, filter F160W. Below each linearity test is the average behavior for the entire quadrant with 2 sigma about the mean.

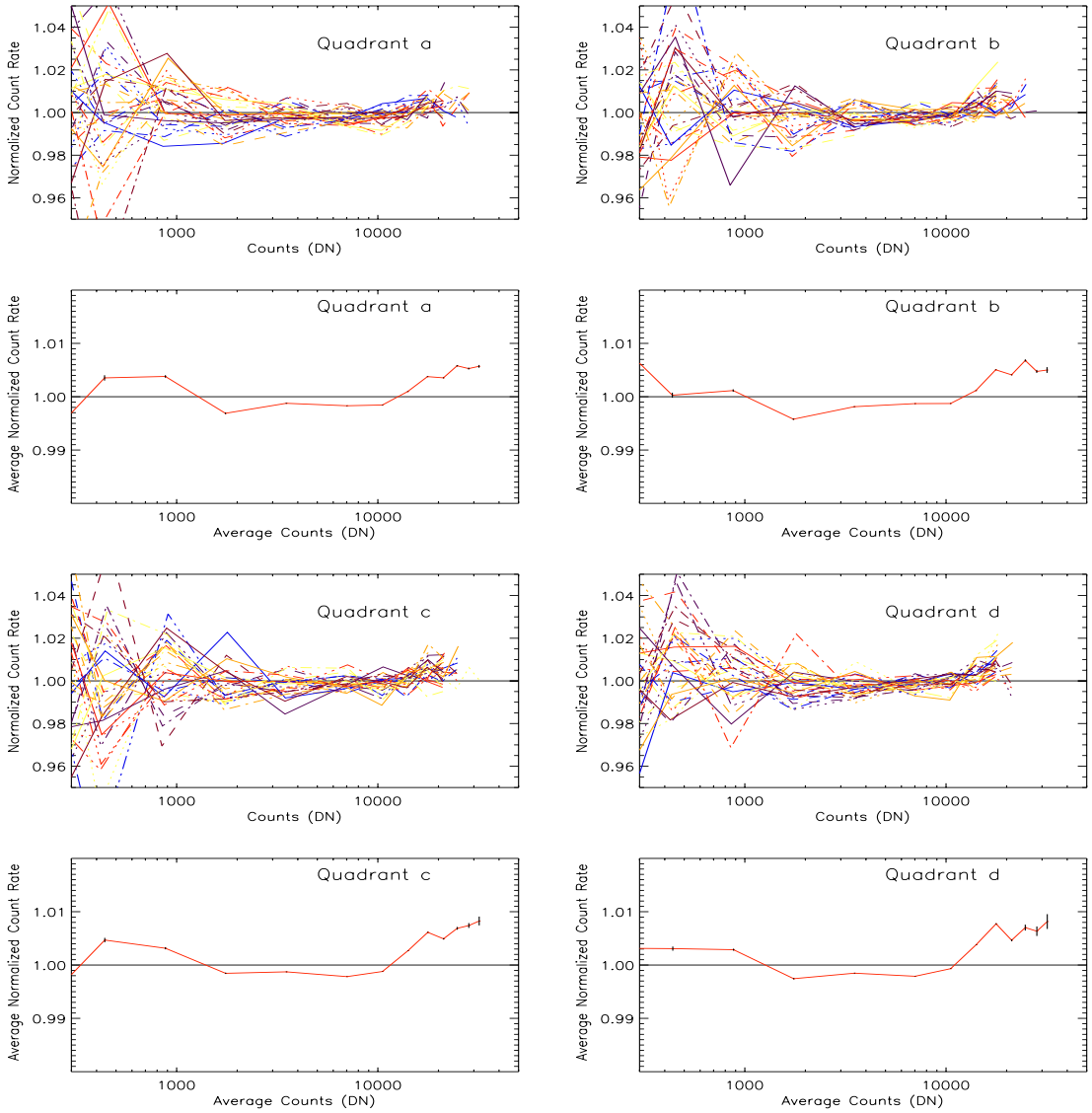

Figure 22: Count Linearity Test for 30 random pixels in each quadrant of a pointed flat field image taken in March 2005 for NIC 1, filter F160W. Below each linearity test is the average behavior for the entire quadrant with 2 sigma about the mean.

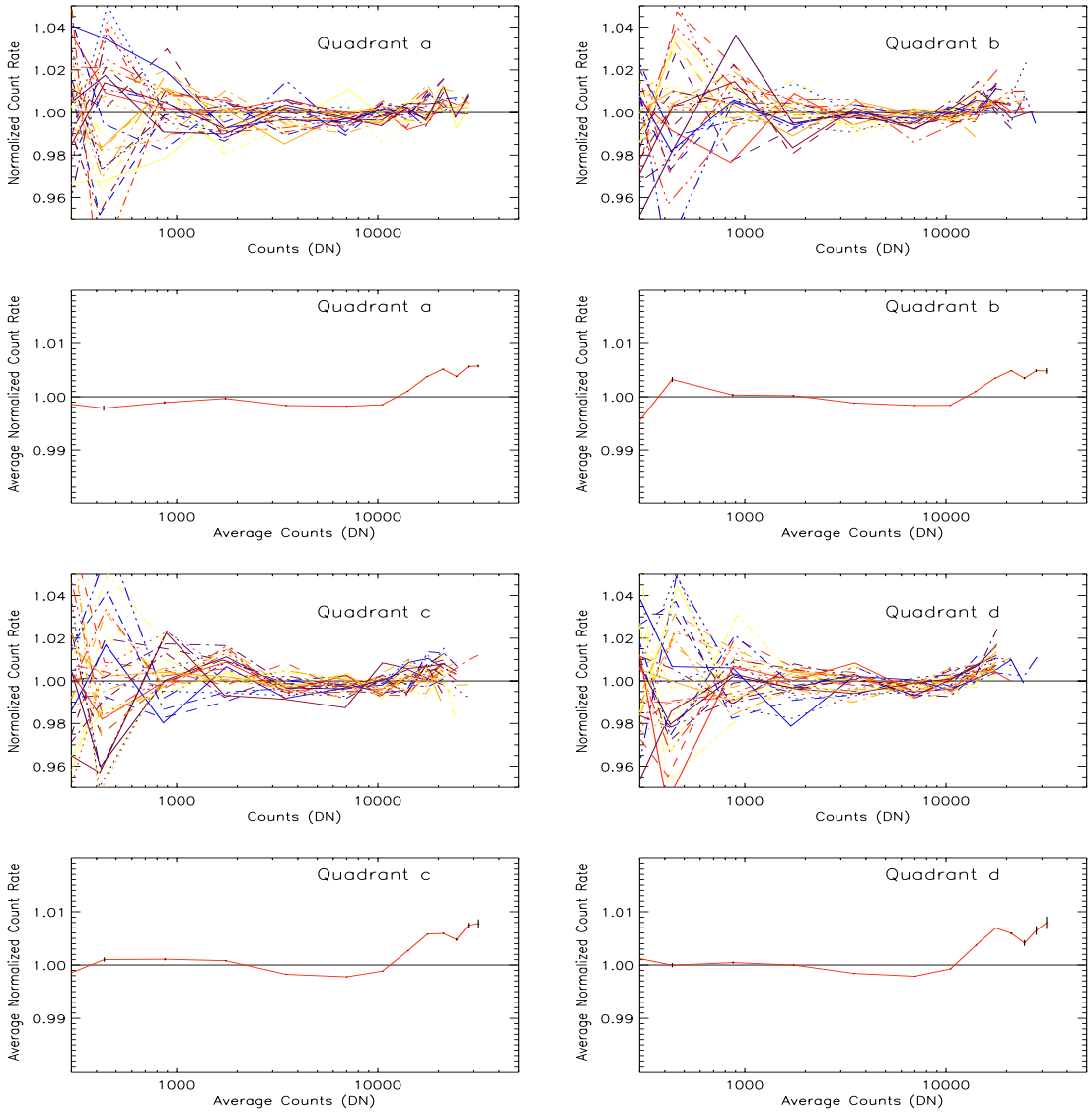

Figure 23: Count Linearity Test for 30 random pixels in each quadrant of a pointed flat field image taken in November 2006 for NIC 1, filter F160W. Below each linearity test is the average behavior for the entire quadrant with 2 sigma about the meaan.